

The procedure used to establish design criteria for band-stop filters utilizing the resonators of Fig. 3 is straightforward. The basic section of the filter of Fig. 1 is considered to be a quarter-wavelength transmission line shunted at its mid-point by a series resonant circuit as shown in Fig. 4. The image parameters of the resonators of Figs. 3 and 4 are then equated. The slope parameter of the shunt series-resonant circuit is then related to the coupling parameter of the parallel coupled lines.

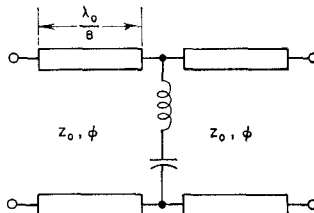


Fig. 4—Basic section of filter in Fig. 1.

For the resonator of Fig. 3 the image parameters are

$$Z_I = Z_0 \sqrt{\frac{\tan^2 \phi - k}{k \tan^2 \phi - 1}}, \quad (1)$$

$$\gamma_I = 2 \tanh^{-1} \left\{ \tan \phi \left[ \frac{1 - k \tan^2 \phi}{\tan^2 \phi - k} \right]^{1/2} \right\}, \quad (2)$$

where

$$k = \sqrt{1 - c^2} \approx 1 - c^2/2 \quad \text{for } c^2 \ll 1, \quad (3)$$

$$c = \frac{Z_{oe} - Z_{oo}}{Z_{oe} + Z_{oo}} = \text{coupling parameter}, \quad (4)$$

$Z_{oe}$  = even-mode characteristic impedance with respect to ground of each conductor.

$Z_{oo}$  = odd-mode characteristic impedance with respect to ground of each conductor.

$\phi$  is defined in Fig. 3.

For the resonator of Fig. 4 the image parameters are

$$Z_I' = Z_0 \sqrt{\frac{\tan \phi (\tan \phi + y)}{y \tan \phi - 1}}, \quad (5)$$

$$\gamma_I' = 2 \tanh^{-1} \tan \phi \left[ \frac{1 - y \tan \phi}{\tan \phi (\tan \phi + y)} \right]^{1/2}, \quad (6)$$

where

$$y = \frac{2}{Z_0} \left( \omega L - \frac{1}{\omega C} \right). \quad (7)$$

Thus if  $Z_I = Z_I'$ , then  $\gamma_I = \gamma_I'$ . Equating the image impedances yields

$$y = \frac{2 - c^2}{c^2} (1 - \cot^2 \phi). \quad (8)$$

The slope parameter of the shunt series-resonant circuit is given by

$$x = \frac{\omega_0}{2} \frac{dX}{d\omega} \Big|_{\omega=\omega_0} \quad (9)$$

and is given in terms of the low-pass prototype elements by Young, *et al.* Using (7) and (8)

$$\frac{dy}{d\omega} \Big|_{\omega=\omega_0} = \frac{4}{\omega_0} \frac{x}{Z_0} \quad (10)$$

$$= \frac{2 - c^2}{c^2} \frac{\pi}{\omega_0}. \quad (11)$$

Therefore,

$$\frac{c^2}{2 - c^2} = \frac{\pi}{4} \left( \frac{Z_0}{x} \right)$$

or

$$c^2 = \frac{\pi \left( \frac{Z_0}{x} \right)}{1 + \frac{\pi}{4} \frac{Z_0}{x}}. \quad (12)$$

Using the expressions for  $x_i$ , the slope parameter for the  $i$ th shunt resonator, given by Young,

$$c_1 = \sqrt{\frac{2\pi\omega_1' g_0 g_1}{4w^{-1} + \pi\omega_1' g_0 g_1}}; \quad (13)$$

$$c_i = \sqrt{\frac{2\pi\omega_1' g_i}{4g_0 w^{-1} + \pi\omega_1' g_i}} \quad \text{for } i\text{-even}, \quad (14)$$

$$c_i = \sqrt{\frac{2\pi\omega_1' g_0 g_i}{4w^{-1} + \pi\omega_1' g_0 g_i}} \quad \text{for } i\text{-odd}. \quad (15)$$

This completes the derivation of the design criteria. Identical results are obtained by considering the behavior of the resonators near resonance, using the expressions for  $L$  and  $C$  given by Young, *et al.*, in terms of the low pass prototype, and satisfying (8). In this case the approximations required are

$$\left( \frac{\omega}{\omega_0} - \frac{\omega_0}{\omega} \right) \approx 2 \left( \frac{\omega - \omega_0}{\omega_0} \right) \quad (16)$$

and

$$\left[ 1 + \frac{\pi}{4} \left( \frac{\omega - \omega_0}{\omega_0} \right) \right]^2 \approx 1 + \frac{\pi}{2} \left( \frac{\omega - \omega_0}{\omega_0} \right). \quad (17)$$

These approximations are quite valid for narrow bandwidth filters.

It should also be noted that a second type of resonator similar to that shown in Fig. 3 may also be used. For the latter the short circuits in Fig. 3 are replaced by open circuits. The design criteria may be developed in a manner similar to the above. However, this type of resonator requires compensation due to fringing at the open circuit ends. In addition some sort of support such as a dielectric post is required which tends to decrease unloaded  $Q$ . Hence, it is believed that the resonator of Fig. 3 is more suitable for practical applications.

Model work on filters of this type will begin shortly.

ROBERT D. STANLEY  
A. C. TODD  
IIT Research Institute  
Chicago, Ill.

## Comments on "Maximum Efficiency of a Two Arm Waveguide Junction"\*

In connection with a recent communication by Beatty<sup>1</sup> I wish to advise you that we have been studying the two-arm dissipative waveguide junction in our laboratory. Two years ago I published<sup>2,3</sup> a new demonstration of Deschamp's method for measuring scattering coefficients and the general properties of those coefficients.

In a recent work, not yet published, we show the variations of the absorbed power against the reflection coefficient of the terminal load.

S. LEFEUVRE  
Ecole Nationale Supérieure d'Electrotechnique, d'Électronique et d'Hydraulique  
Université de Toulouse, France

\* Received July 22, 1963.

<sup>1</sup> R. W. Beatty, "Maximum efficiency of a two arm waveguide junction," *IEEE TRANS. ON MICROWAVE THEORY AND TECHNIQUES (Correspondence)*, vol. MTT-11, p. 94, January, 1963.

<sup>2</sup> S. Lefèuvre, "Détermination de l'impédance caractéristique d'un quadripôle quelconque en hyperfréquences," *Compt. Rend. Acad. Sci.*, vol. 250, pp. 3288-3289, 1960.

<sup>3</sup> S. Lefèuvre, "Quelques propriétés des quadripôles dissipatifs en hyperfréquences," *Compt. Rend. Acad. Sci.*, vol. 252, pp. 4135-4136, 1961.

## A Uniform Coaxial Line with an Elliptic-Circular Cross Section\*

Analysis and design of a nonuniform coaxial line with an isoperimetric sheath deformation has been reported.<sup>1</sup> The object of this note is to show that the procedure followed therein can be adopted for evaluating some of the essential features of an infinitely long ideal transmission line with an elliptic sheath and a circular inner conductor. Apart from its reported use with the nonuniform line, this type of structure may also be found in medium and large sized electro-nuclear machines.<sup>2</sup>

### I. LINE CONSTANTS

Eqs. (15)-(21) in the communication quoted<sup>1</sup> provide expressions for the primary and the secondary constants of the line as follows:

$$\text{Capacitance per unit length} = C = \frac{4\pi\epsilon}{G} \quad (1a)$$

External inductance per unit length

$$= L^* = \frac{\mu G}{4\pi} \quad (1b)$$

Characteristic impedance

$$= Z_0 = \frac{G}{4\pi} \sqrt{\frac{\mu}{\epsilon}} \quad (2a)$$

\* Received March 11, 1963; revised manuscript received July 23, 1963.

<sup>1</sup> N. Seshagiri, "A non-uniform line with an isoperimetric sheath deformation," this issue, page 478.

<sup>2</sup> P. M. Morse and H. Feshbach, "Methods of Theoretical Physics," McGraw-Hill Book Co., Inc., New York, N. Y., p. 1204; 1953.

The phase constant  $\beta = \omega\sqrt{\epsilon\mu}$ . (2b)

## II. TEM WAVE EQUATION

The approximate equations representing the TEM wave are derived in four steps. First, the expressions for the rms electric and magnetic field strengths for an infinite uniform line having a circular eccentric outer conductor is given. Then, these equations are remodeled in the polar form with the origin reckoned at the center of the inner conductor. Next, two compensations, *viz.*, a radial coordinate shrinking and an equivalent capacitance are described. Finally, the effect of these two compensations are superposed on the polar equation given by the second step to get the resultant expression for the TEM wave.

### A. Structure with a Circular Eccentric Outer Conductor

Fig. 1 shows a simple, nonlinear transformation of a half-plane structure in the  $Z$  plane consisting of a half ellipse and a semi-circle, by an analytic relation,

$$W = Z^2. \quad (3)$$

The transformed structure in the  $W$  plane is an ellipse of lesser eccentricity than that of the original structure. By the properties of the transformation, the following relations are applicable:

$$\begin{aligned} a_1 &= \frac{1}{2}(a_0^2 + b_0^2) \\ e_1 &= \frac{1}{2}(a_0^2 - b_0^2) \\ r_1 &= r_0^2. \end{aligned} \quad (3a)$$

For the case of the auxiliary circle about the displaced transformed elliptic sheath of Fig. 1(b), the electric and magnetic fields can be mapped using the bipolar coordinates<sup>3,4</sup> ( $u, v, z$ ) and it can be shown that,

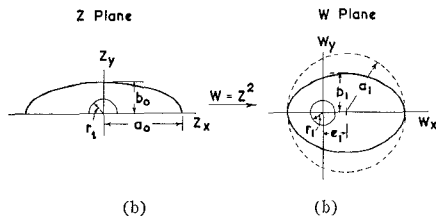


Fig. 1—Transformation of the half structure of the elliptic-circular coaxial line into a noncoaxial elliptic-circular configuration.

$$\begin{aligned} \left\{ \begin{array}{l} E_{\text{rms}} \\ H_{\text{rms}} \end{array} \right\} &= \left\{ \begin{array}{l} \mathbf{a}_u \\ \mathbf{a}_v \\ \eta_0 \end{array} \right\} \\ &\cdot \frac{V_{\text{rms}}(\cosh u - \cos v)e^{-j\beta z}}{a_r(u_2 - u_1)}. \end{aligned} \quad (4)$$

Here,

$E_{\text{rms}}$  = rms electric field strength (complex),

$H_{\text{rms}}$  = rms magnetic field strength (complex),

$\mathbf{a}$  = unit vector,

<sup>3</sup> P. Moon and D. E. Spencer, "Cylindrical and rotational coordinate system," *J. Franklin Inst.*, vol. 252, pp. 327-343; October, 1951.

<sup>4</sup> P. Moon and D. E. Spencer, "TEM wave in cylindrical systems," *J. Franklin Inst.*, vol. 256, pp. 325-353; October, 1953.

$V_{\text{rms}}$  = rms voltage at ( $z=0$ ),  
 $z$  = distance along the  $z$ -axis,  
 $u_1, u_2 = u$  at the outer, inner boundary,  
 $\eta_0$  = intrinsic impedance,

and

$$\begin{aligned} a_r &= \frac{1}{2e_1} [e_1^4 - 2e_1^2(a_1^2 + r_1^2) \\ &\quad + (a_1^2 - r_1^2)^2]^{1/2}. \end{aligned} \quad (4a)$$

### B. Polar Form

The compensations that are deduced in the next step necessitate the conversion of (4) into the polar form with the origin reckoned at the center of the transformed inner conductor instead of the geometric center of the bipolar coordinate. If  $(r, \theta, z)$  refers to the transformed structure of Fig. 1(b), then,

$$\left\{ \begin{array}{l} E_{\text{rms}} \\ H_{\text{rms}} \end{array} \right\} = \left\{ \begin{array}{l} \mathbf{a}_u \\ \mathbf{a}_v \\ \eta_0 \end{array} \right\} \frac{2a_r V_{\text{rms}} e^{-j\beta z}}{(u_2 - u_1)\sqrt{D}} \quad (5)$$

where,

$$\begin{aligned} D &= (r^2 + w_1^2 + 2rw_1 \cos \theta)^2 + a_r^4 \\ &\quad - 2a_r^2(r^2 \cos 2\theta + w_1^2 + 2rw_1 \cos \theta) \end{aligned} \quad (6)$$

$$w_1 = \sqrt{a_r^2 + r_1^2}. \quad (6a)$$

In (5)  $(u_2 - u_1)$  is retained with the same meaning as conveyed by (4) for a future identification of this with a term in an equivalent capacitance. Also, the subscripts  $u$  and  $v$  in the unit vector of (5) are related to the expressions

$$u = \sinh^{-1} \left[ \frac{2a_r(r \cos \theta + w_1)}{\sqrt{D}} \right] \quad (7a)$$

$$v = \sin^{-1} \left[ \frac{2a_r r \sin \theta}{\sqrt{D}} \right]. \quad (7b)$$

### C. Compensations

Two compensations are considered: a radial shrinking from the standpoint of boundary conditions, and an equivalent capacitance based on field considerations.

$$r_e = \frac{b_1^2 e_1 \cos \theta + a_1 b_1 [(a_1^2 - e_1^2) \sin^2 \theta + b_1^2 \cos^2 \theta]^{1/2}}{b_1^2 \cos^2 \theta + a_1^2 \sin^2 \theta}. \quad (8b)$$

#### 1) Radial Coordinate Shrinking:

For  $1 < a_0/b_0 < 2.5$ , as shown earlier, the transformation given by (3) maps the elliptic outer conductor into a nearly circular one. It will be shown presently on the basis of an experiment that using an approximate method the field map obtained from the eccentric circular cylinders can be adopted to draw the field map for a nearly circular eccentric outer. This will be effected in such a way that on the surface of the inner conductor there will be no change in the field configuration, while at the other boundary, the auxiliary circle will be identified with the nearly circular ellipse.

Fig. 2 gives the electric lines of force and potential lines for the displaced ellipse and its auxiliary circle in the  $W$  plane, being the result of an electrostatic experiment performed for a representative case in which

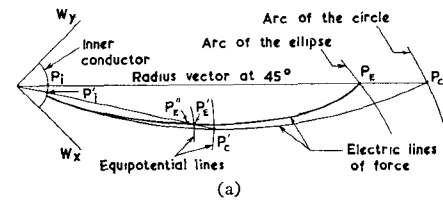


Fig. 2—Field map for deriving a radial shrinking compensation from an electrostatic experiment.

$a_0 = 2b_0$  and  $r_i = 0.5 b_0$ . The electric lines of force, terminating at equipotential points  $P_E$  and  $P_C$  on the periphery of the ellipse and the circle, each taken one at a time, are traced for two representative radii vectors at  $45^\circ$  and  $90^\circ$ . For an intermediate value of the potential, a second set of equipotential lines are identified. The point  $P_C'$  is the intersection of the electric line and the equipotential line for the circular case and  $P_E'$  for the elliptic case. If a point  $P_E''$  is marked on the radial line obtained by a linear shrinking of  $P_i'P_C'$  equal to  $P_EP_i/P_C'P_i$ , it can be observed from Fig. 2 that  $P_E''$  is very close to the near trijunction of the electric line, the potential line and the radial line taken with respect to the ellipse. This ratio is expressed as

$$R = \frac{r_e - r_1}{r_e - r_i} \quad (8)$$

where

$$r_e = c_1 \cos \theta + (a_1^2 - e_1^2 \sin^2 \theta)^{1/2}, \quad (8a)$$

and

$$r_i = c_1 \cos \theta + (a_1^2 - e_1^2 \sin^2 \theta)^{1/2}. \quad (8b)$$

#### 2) Equivalent Capacitance:

Ellipticity of the transformed outer conductor causes an intensification of the equipotential surfaces than that corresponding to the auxiliary cylinder. This is equivalent to an increase in the static capacity. From (4) it has been shown by Moon and Spencer<sup>5</sup> that

$$(u_1 - u_2) = P/C_0 \quad (9)$$

where  $P$  is a constant and  $C_0$  is the capacitance. Also, from (4) and (9) the term  $(C_0 V_{\text{rms}}/P a_r)$  stands for a magnitude where  $C_0/d_r$  depends upon the structure. The rest of the terms in (4), however, stand for the position and the direction of the magnitude.

<sup>5</sup> P. Moon and D. E. Spencer, "Field Theory for Engineers," D. Van Nostrand Inc., Princeton, N. J., pp. 366-368; 1961.

A capacitance equivalent to  $C_0$ , when the outer structure has a near circularity, is given by (1a).

#### D. Superposition

It will now be assumed that, when the transformed structure does not deviate far from circularity, the two compensations can be applied mutually independent of each other. This is because the first compensation is positional, while the second is one of magnitude. Thus, superposing the two compensations in (5) and considering polar coordinates  $(\eta, \Theta, z)$  with respect to the original structure in the  $Z$  plane, the following expression describing the TEM wave is obtained

$$\left\{ \begin{array}{l} E_{\text{rms}} \\ H_{\text{rms}} \end{array} \right\} = \left\{ \begin{array}{l} a_{u'} \\ a_{v'} \\ \eta_0 \end{array} \right\} \frac{4a_r V_{\text{rms}} e^{-j\beta z}}{(-G)\sqrt{D'}}. \quad (10)$$

Here, if (6) to (8) are represented in the form,

$$u, v, D = F_1, F_2, F_3(r, \theta)$$

and

$$R = \frac{F_e(\theta) - r_1}{F_e(\theta) - r_1}$$

then,

$$u', v', D' = F_1, F_2, F_3$$

$$\cdot \left[ \left( \frac{\eta^2 + R' r_1 - r_1}{R'} \right), 2\Theta \right]$$

and

$$R' = \frac{F_e(2\Theta) - r_1}{F_e(2\Theta) - r_1}$$

#### III. FORCE ON THE INNER CONDUCTOR

From the properties of the transformation (3) and the bipolar coordinate,<sup>5</sup> the magnitude of a force acting on the inner conductor can be deduced.

$$F = \frac{dw}{de_1} = \frac{\pi \epsilon V^2}{a_r G^2} \quad (11)$$

where

$F$  = force per unit length of the line,  
 $w$  = energy stored in the electric field,  
 $V$  = voltage difference between the inner and the outer conductors.

A one-to-one correspondence shows that forces  $\vec{F}$  and  $\vec{F}$  act on the inner conductor for the full structure along the minor axis of the ellipse in a direction tending to compress the former. The resultant displacement of the inner conductor from the geometric center of the ellipse, in conformity with quarter symmetry, is zero, by virtue of the equal and opposite nature of  $\vec{F}$  and  $\vec{F}$ .

N. SESHAGIRI  
 Dept. Electrical Communication  
 Engineering  
 Indian Institute of Science,  
 Bangalore, India

#### Discontinuity Effects in Single Resonator Traveling Wave Filters\*

In a previous correspondence the exact frequency response of the single resonator traveling wave directional filter was presented assuming that all transmission lines had characteristic impedances equal to the terminating impedance of the network.<sup>1</sup> The purpose of this correspondence is to extend the previous work to take into account the case where the transmission lines connecting the parallel coupled lines have an arbitrary characteristic impedance  $Z_I$ . The resulting structure is shown in Fig. 1.

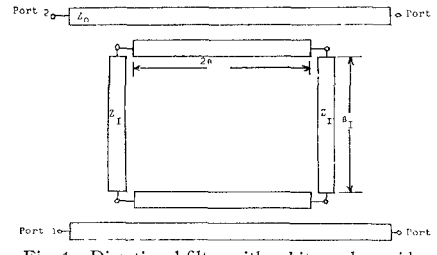


Fig. 1—Directional filter with arbitrary loop sides.

The symmetric-asymmetric excitation analysis is applied as discussed in the previous correspondence, with the transmission line matrix representing the loop sides plus corner equivalents replaced by

$$\begin{vmatrix} \cosh \alpha_I & Z_I \sinh \alpha_I \\ \hline \hline \sinh \alpha_I & \cosh \alpha_I \\ \hline \hline Z_I & \end{vmatrix}.$$

In general  $\alpha_I = j\beta_I$ , and  $Z_I$  will be real so that the above becomes

$$\begin{vmatrix} \cos \beta_I & jZ_I \sin \beta_I \\ \hline \hline j \frac{\sin \beta_I}{Z_I} & \sin \beta_I \\ \hline \hline Z_I & \end{vmatrix}.$$

Making this change, carrying out the matrix multiplication, and calculating the transfer and reflection coefficients there is obtained,

$$\begin{aligned} T_S = 2 \left\{ \left[ 2 \left( \cosh 2\alpha \cos \beta_I + \frac{\sin \beta_I \sinh 2\alpha}{2} \right. \right. \right. \\ \cdot \left( \frac{Z_0}{Z_I} \cot \theta - \frac{Z_I}{Z_0} \tan \theta \right) \left. \right) \left. \right] \\ + j \left[ \sin \beta_I \left( \left( \frac{Z_0}{Z_I} + \frac{Z_I}{Z_0} \right) \cosh^2 \alpha \right. \right. \\ \left. \left. - \sinh^2 \alpha \left( \frac{Z_I}{Z_0} \tan^2 \theta + \frac{Z_0}{Z_I} \cot^2 \theta \right) \right) \right. \\ \left. \left. + \cos \beta_I \sinh 2\alpha (\tan \theta - \cot \theta) \right] \right\}^{-1} \end{aligned} \quad (1)$$

\* Based on part of the research work undertaken by Robert D. Standley in partial fulfillment of the requirements for the Ph.D. degree at Illinois Institute of Technology; Chicago, Ill.

<sup>1</sup> R. D. Standley, "Frequency response of strip traveling wave directional filters," IEEE TRANS. ON MICROWAVE THEORY AND TECHNIQUES, vol. 11, pp. 264-265; July, 1963.

$$\begin{aligned} T_A = 2 \left\{ \left[ 2 \left( \cosh 2\alpha \cos \beta_I + \frac{\sin \beta_I \sinh 2\alpha}{2} \right. \right. \right. \\ \cdot \left( \frac{Z_I}{Z_0} \cot \theta - \frac{Z_0}{Z_I} \tan \theta \right) \left. \right) \left. \right] \\ + j \left[ \sin \beta_I \left( \left( \frac{Z_0}{Z_I} + \frac{Z_I}{Z_0} \right) \cosh^2 \alpha \right. \right. \\ \left. \left. - \sinh^2 \alpha \left( \frac{Z_I}{Z_0} \cot^2 \theta + \frac{Z_0}{Z_I} \tan^2 \theta \right) \right) \right. \\ \left. \left. + \cos \beta_I \sinh 2\alpha (\tan \theta - \cot \theta) \right] \right\} \end{aligned} \quad (2)$$

$$\begin{aligned} \Gamma_S = j \frac{T_S}{2} \left\{ \sin \beta_I \left[ \left( \frac{Z_I}{Z_0} - \frac{Z_0}{Z_I} \right) \cosh^2 \alpha \right. \right. \\ \left. \left. - \sinh^2 \alpha \left( \frac{Z_0}{Z_I} \cot^2 \theta - \frac{Z_I}{Z_0} \tan^2 \theta \right) \right] \right. \\ \left. - \cos \beta_I \sinh 2\alpha (\cot \theta + \tan \theta) \right\} \end{aligned} \quad (3)$$

$$\begin{aligned} \Gamma_A = j \frac{T_A}{2} \left\{ \sin \beta_I \left[ \left( \frac{Z_I}{Z_0} - \frac{Z_0}{Z_I} \right) \cosh^2 \alpha \right. \right. \\ \left. \left. + \sinh^2 \alpha \left( \frac{Z_I}{Z_0} \cot^2 \theta - \frac{Z_0}{Z_I} \tan^2 \theta \right) \right] \right. \\ \left. + \cos \beta_I \sinh 2\alpha (\cot \theta + \tan \theta) \right\} \end{aligned} \quad (4)$$

where

$$\cosh \alpha = \frac{Z_{0e} + Z_{00}}{Z_{0e} - Z_{00}}$$

and the other symbols are defined in Fig. 1. Hence in the general case where  $Z_I \neq Z_0$ ,

$$T_A \neq T_S$$

$$\Gamma_A \neq \Gamma_S.$$

Referring to the equations for the output voltages, the above results mean that:

- 1) A finite reflection will result at port 1.
- 2) Port 3 is not isolated.
- 3) A Butterworth response will not result at port 2.

In order to show the above more conclusively and to obtain an idea as to the effect of the ratio  $Z_I/Z_0$ , (1) through (4) were used to calculate the network response. Loaded  $Q$  values of 50 and 100 were used with  $Z_I/Z_0$  as a parameter. It was also assumed that  $2\theta = \beta_I$ . The results of the calculations are plotted in Figs. 2-5 for  $Q_L = 100$ .

It is important to note that the computed results predict the experimentally observed fact that a misaligned filter of this type yields a double resonance response shape.

To obtain a knowledge of the effect of  $\beta_I$ , the responses were calculated with  $2\theta/\beta_I = k$  as a parameter. It was assumed that  $\beta_I$  would have a linear frequency dependence over the limited range of electrical angle of the calculations. The results were plotted and it was found that the primary effect of having  $k \neq 1$  is to shift the resonant frequency to

$$f = \frac{k}{k+1} f_0$$

where it has been assumed that

$$2\theta = \frac{\pi}{2} \frac{f}{f_0}.$$